*Plant, Cell and Environment* (2006) **29**, 1298–1308 doi: 10.1111/j.1365-3040.2006.01508.x

# Thermal history regulates methylbutenol basal emission rate in *Pinus ponderosa*

DENNIS W. GRAY[1], ALLEN H. GOLDSTEIN[2] & MANUEL T. LERDAU[3]

[1]*Department of Ecology and Evolutionary Biology, University of Connecticut, 75 North Eagleville Road, Storrs, CT 06269-3043,* [2]*Department of Environmental Science, Policy and Management (ESPM), University of California at Berkeley, 151 Hilgard Hall, Berkeley, CA 94720, and* [3]*Department of Ecology and Evolution, State University of New York, Stony Brook, NY 11794-5245, USA*

## ABSTRACT

**Methylbutenol (MBO) is a 5-carbon alcohol that is emitted by many pines in western North America, which may have important impacts on the tropospheric chemistry of this region. In this study, we document seasonal changes in basal MBO emission rates and test several models predicting these changes based on thermal history. These models represent extensions of the ISO G93 model that add a correction factor $C_{basal}$, allowing MBO basal emission rates to change as a function of thermal history. These models also allow the calculation of a new emission parameter $E_{standard30}$, which represents the inherent capacity of a plant to produce MBO, independent of current or past environmental conditions. Most single-component models exhibited large departures in early and late season, and predicted day-to-day changes in basal emission rate with temporal offsets of up to 3 d relative to measured basal emission rates. Adding a second variable describing thermal history at a longer time scale improved early and late season model performance while retaining the day-to-day performance of the parent single-component model. Out of the models tested, the $T_{amb}$,$T_{max7}$ model exhibited the best combination of day-to-day and seasonal predictions of basal MBO emission rates.**

*Key-words*: 2-methyl-3-buten-2-ol; emissions algorithm; isoprene; MBO; temperature history; thermal protection; VOC emission modelling.

## INTRODUCTION

Plants produce and emit into the atmosphere a diverse array of volatile organic compounds (VOCs) including methanol (MacDonald & Fall 1993b; Nemecek-Marshall *et al*. 1995) ethanol (Kreuzweiser, Schnitzler & Steinbrecher 1999), acetone (MacDonald & Fall 1993a; Goldstein & Schade 2000) and hydrocarbons such as isoprene and monoterpenes (Kreuzweiser *et al*. 1999). The production and release of these VOCs represents an important means through which plants exert profound influences on the trace gas composition of the atmosphere and the chemical processes taking place in the troposphere. These reactive VOCs have been implicated in a host of atmospheric processes including the production of tropospheric ozone (Brasseur & Chatfield 1991; Chameides *et al*. 1992; Fehsenfeld *et al*. 1992); the regulation of OH radical concentration in the troposphere (Ehhalt, Dorn & Poppe 1991), and in contributing to the formation of aerosols (Novakov & Penner 1993; Andreae & Crutzen 1997). Phytogenic VOCs may also indirectly exacerbate the greenhouse effects of methane by increasing its residence time in the atmosphere (Jacob & Wofsy 1988; Wuebbles *et al*. 1989). Thus, identifying the processes regulating VOC emission to the atmosphere and predicting the magnitude of emission under various environmental conditions is an important prelude to understanding and predicting the chemical behaviour of the lower atmosphere.

Globally, isoprene and the monoterpenes are by far the most important and well-studied VOCs (Tingey *et al*. 1979; Zimmerman 1979; Tingey, Evans & Gumpertz 1981; Monson & Fall 1989; Harley *et al*. 1994; Monson *et al*. 1994; Harley, Guenther & Zimmerman 1996). Isoprene emission from plants is estimated to represent inputs of as much as 452 Tg of reactive carbon into the atmosphere annually (Guenther *et al*. 1995). Recently, a C-5 alcohol, 2-methyl-3-buten-2-ol (methylbutenol or MBO), was discovered to be emitted in large amounts from many pines in western North America (Goldan, Kuster & Fehsenfeld 1993; Harley *et al*. 1998), and has been shown to have impacts rivalling those of isoprene and monoterpenes in large portions of this region (Harley *et al*. 1998; Lamanna & Goldstein 1999).

The emission of many VOCs responds strongly to both light and temperature in a fashion that depends on whether the VOC is emitted immediately upon production (e.g. isoprene and MBO) or resides in a storage reservoir within the plant's tissues (e.g. monoterpenes). VOCs that are not stored, such as MBO, exhibit an Arrhenious temperature response where emission increases exponentially to a temperature optimum above which emissions decline precipitously. Non-stored VOCs respond asymptotically to light, increasing rapidly from low light intensities towards a plateau at high light (Tingey *et al*. 1979; Monson *et al*. 1991,

*Correspondence: Dennis W. Gray. Fax: +1 860 486 6364; e-mail: dennis.gray@uconn.edu*

1992; Loreto & Sharkey 1993; Harley *et al*. 1998; Gray, Lerdau & Goldstein 2003).

These responses of VOC emission to light and temperature take place on a time scale of seconds to minutes and have thus been termed 'instantaneous' (Guenther, Monson & Fall 1991; Guenther, Zimmerman & Harley 1993). By holding light and temperature constant during a measurement period, such instantaneous responses are factored out and one obtains an emission rate that is defined for a specific set of light and temperature conditions. This emission rate measured under a standard set of light and temperature conditions has received many names. It is referred to most commonly as a 'basal' emission rate or 'BER' (Guenther *et al*. 1993), although also as a 'standard emission rate' or 'SER' (Lerdau & Gray 2003), an 'emission factor' (Guenther 1997) or an 'emission capacity' (Harley, Guenther & Zimmerman 1997). Regardless of the name applied to this emission rate, a basal emission rate represents one of the basic parameters used in models to predict VOC emission.

Basal emission rates are typically viewed as representing the inherent capacity of a plant to produce a particular VOC. Initially, models used to predict VOC emission rates assumed that basal emission rates were constant and applied light and temperature correction factors to model changes in VOC emission caused by the 'instantaneous' effects of light and temperature (Guenther *et al.* 1993). However, it has become increasingly apparent that basal emission rates may change over time (Goldstein *et al*. 1998; Llusià & Peñuelas 2000; Gray *et al*. 2003; Kuhn *et al*. 2004).

Numerous attempts have been made to correct for changing basal emission rates in VOC emission models. The simplest of these involves applying new empirically derived basal emission rate estimates as the season progresses (Schade *et al*. 2000) or modelling changes in basal rates as a function of time (Guenther 1997). A similar approach was taken by Schnitzler, Lehning & Steinbrecher (1997) who used the seasonal pattern of extractable isoprene synthase activity to model seasonal changes in isoprene basal emission rates. However, such empirical approaches carry the drawback that the resulting models may not generalize to other data sets, locations, and time periods.

Evidence from leaf-level measurements and tower flux studies increasingly suggests that changes in basal isoprene emission rate are driven by thermal history (Fuentes & Wang 1999; Sharkey *et al*. 1999; Geron *et al*. 2000; Lehning *et al*. 2001; Pétron *et al*. 2001). Monson *et al*. (1994) showed that isoprene emission began earlier in aspen leaves grown at high temperature, Sharkey & Loreto (1993) showed that nonemitting (young) Kudzu leaves could be induced to produce isoprene following a 5 h exposure at 30 °C, and Gray *et al*. (2003) has shown that basal MBO emission rates are strongly correlated with ambient temperature. Several authors have tried to model changes in isoprene basal emission rates as a function of light or temperature (Fuentes & Wang 1999; Sharkey *et al*. 1999; Geron *et al*. 2000; Lehning *et al*. 2001); however, these models have generally overestimated emissions in early and late season (Monson *et al*. 1994; Schnitzler *et al*. 1997; Fuentes & Wang 1999).

In this paper, we examine the relationship between thermal history and MBO basal emission rate observed in MBO emission data collected from ponderosa pine in 1998 and 2000. From the data collected in 2000 we construct several models describing changes in MBO basal emission as a function of thermal history and test these models against MBO emission data collected in 1998. These models are implemented as a correction term $C_{basal}$ for the ISO G93 algorithm (Guenther *et al.* 1993). The ISO G93 model traces its origins to work by Zimmerman (1979) and predicts leaf-level instantaneous VOC emission rates using basal VOC emission rates, light intensity and leaf temperature as model inputs. Including the $C_{basal}$ term provides a means to correct for changes in basal emission rates known to take place over longer time intervals and replaces empirical estimates of basal MBO emission rates with an algorithm for predicting changes in basal emission rates as a function of thermal history.

## METHODS

### Study site and species

Experiments were conducted in the central Sierra Nevada Mountains of California at the UC Berkeley Blodgett Forest Research Station and on an adjacent property owned by Sierra Pacific Industries. Blodgett Forest Research Station is located east of the town of Georgetown, CA at an elevation of 1300 m (38°53′42.9″N, 120°37′57.9″W). This region experiences a Mediterranean climate, with hot dry summers and cool wet winters. Studies took place at two sites in even-aged plantations of ponderosa pine (*Pinus ponderosa* Dougl. ex Laws.*)* that also contained scattered individuals of sugar pine (*Pinus lambertiana* Dougl.), Douglas fir [*Pseudostuga menziesii* (Mirb.) Franco], white fir [*Abies concolor* (Gord. & Glend.) Hildebr.] and incense cedar (*Calocedrus decurrens* Torr.). In 1998 studies took place in an even-aged plantation of ponderosa pine (*P. ponderosa* Dougl. ex Laws.), aged 7–8 years and 3–5 m in height, owned by Sierra Pacific Industries. A micrometeorological tower located at this site provided detailed climate records for this site throughout the sampling period. In 2000, studies took place in an even-aged plantation of ponderosa pine, aged 10–15 years and 4–6 m in height, located in compartment 400 of Blodgett Forest Research Station. This site was located on a south-east facing slope and also contained scattered individuals of sugar pine (*P. lambertiana* Dougl.), Douglas fir [*P. menziesii* (Mirb.) Franco], white fir [*A. concolor* (Gord. & Glend.) Hildebr.], incense cedar (*C. decurrens* Torr.) and giant sequoia (*Sequoia giganteum*). Temperature data at this site was recorded using portable data loggers. We conducted all experiments on ponderosa pine because it produces large quantities of MBO, covers extensive areas of the forested western United States and is the most commercially important MBO-emitting species.

## Temperature measurements

Measurements of needle temperature were made using four single channel automated data loggers (MicroDAQ, Warner, NH, USA) equipped with 0.005″ (0.127 mm) fine-wire type E thermocouples (Omega Engineering Inc., Stamford CT, USA). To ensure accurate measurement of needle temperature, each thermocouple was wrapped tightly around its associated needle such that the thermocouple junction was tightly appressed to the needle surface. The integrity of this configuration was checked weekly and adjusted as needed, and has proved very robust to disturbances caused by wind induced branch movements.

## Gas exchange and chromatography protocols

Leaf level measurements of photosynthetic variables and MBO emission rates were made using a LiCor LI-6400 portable gas exchange system (Li-Cor Inc., Lincoln, NE, USA) and a Voyager portable gas chromatograph (GC) (PE Photovac Inc., Norwalk, CT, USA). The LI-6400 allows good control of the light, temperature and $CO_2$ environment experienced by the foliage being measured. Light control in this system is achieved with a series of red and blue light-emitting diodes (peak irradiance 665 nm and 470 nm) mounted on top of the leaf cuvette. Temperature is regulated using thermoelectric Peltier coolers mounted on the sides of the cuvette. The Peltier coolers supplied by the manufacturer allow temperature control of the cuvette in a range of ± 6 °C of ambient temperature; however, by adding heating elements in a cardboard shroud enclosing the lower portions of the cuvette, we were able to operate at temperatures as much as 15 °C above ambient. Leaf temperatures were calculated based on the energy balance equations implemented in the LI-6400 software (Li-Cor 1995). The Voyager GC contains three columns and a 1 mL sample loop, operates isothermally, and uses a photoionization detector for detection and quantification of volatiles.

A pair of 1-year-old three-needle fascicles (6 needles) was clamped into the LI-6400 cuvette, and the cuvette flushed with 100 $\mu$mol $s^{-1}$ of ambient air scrubbed of hydrocarbons by passage through an activated charcoal filter. Exhaust gases from the cuvette were routed via Teflon tubing past the sample inlet port on the GC. The GC sample loop was loaded via an internal sampling pump, and a 1 mL aliquot was injected onto a methyl silicone capillary column (15 m length, ID 0.32 mm, coating thickness 12 microns). The GC was operated isothermally at 65 °C and 103.42 kPa column pressure of Ultra High Purity nitrogen carrier gas (Sierra Airgas, Sacramento, CA, USA). The detection limit for this system was 5 p.p.b., and precision was within 10%. Chamber air typically had mixing ratios between 10 and 100 p.p.b. Five-point standard curves diluted from a 100 p.p.m. gas standard (Scott-Marrin, Inc. Riverside, CA, USA) were run at the end of each sampling day.

## Basic model description

We constructed and evaluated a model that extends the ISO G93 algorithm (Guenther *et al*. 1993), as parameterized for MBO emission by Harley *et al*. (1998). This extension adds a correction factor that allows MBO basal emission rates to change as a function of the thermal history experienced by the emitting foliage. In the ISO G93 algorithm the emission rate at any given time under ambient conditions ($E_{amb}$) is a function of a basal emission rate ($E_{basal}$), to which is multiplied a light ($C_L$) and a temperature ($C_T$) correction factor. These correction factors re-scale emission rates to ambient conditions (Eqn 1). A basal emission rate ($E_{basal}$) is an emission rate realized under pre-defined but constant light and temperature conditions during the measurement period. By convention basal emissions are defined as 30 °C and 1000 $\mu$mol photons $m^{-2}$ $s^{-1}$ for isoprene (Guenther *et al.* 1993), and either 1000 $\mu$mol photons $m^{-2}$ $s^{-1}$ (Harley *et al.* 1998) or 1500 $\mu$mol photons $m^{-2}$ $s^{-1}$ (Gray *et al.* 2003) for MBO. In Eqn 1, $E_{basal}$ is treated as constant. To allow for changes in $E_{basal}$ we modify Eqn 1 by including a basal emission rate correction factor ($C_{basal}$), and replace the $E_{basal}$ term with the term $E_{standard30}$ to obtain the model described in Eqn 2. $E_{standard30}$ is the basal emission rate predicted to occur from a plant experiencing a constant temperature history of 30 °C when measured under 1500 PAR at 30 °C. Thus, $E_{standard30}$ represents the inherent VOC production capacity of a plant that is independent of environmental conditions. $C_{basal}$ is a correction factor that adjusts $E_{standard30}$ for changes in temperature history. $E_{standard30}$ and $E_{basal}$ are related through $C_{basal}$ as shown in Eqn 3.

$$E_{amb} = E_{basal}\, C_L C_T \quad (1)$$

$$E_{amb} = E_{standard30}\, C_L C_T C_{basal} \quad (2)$$

$$E_{basal} = E_{standard30}\, C_{basal} \quad (3)$$

## Basal emission rate correction factor ($C_{basal}$) models

We investigated two broad classes of models (single-component and two-component) describing changes in $C_{basal}$ (and hence $E_{basal}$) as a function of the thermal history experienced by the needles of *P. ponderosa*. Single component models examined the impacts of thermal history on one timescale. Most of the single-component models followed the form of Eqn 4 where $\alpha$ and $\beta$ are constants, $T_{hist}$ is a measure of the past thermal history, experienced by a set of needles, $T_{ref}$ is a reference temperature set at 30 °C, $E_{basal}$ is the emission rate obtained under standard measurement conditions (1500 $\mu$mol photons $m^{-2}$ $s^{-1}$ and 30 °C) without controlling for thermal history. $E_{standard30}$ is the basal emission rate expected following a constant temperature history of 30 °C.

$$C_{basal} = \alpha(T_{hist} - T_{ref}) + C = \frac{E_{basal}}{E_{standard30}} \quad (4)$$

We used least squares linear regression to construct linear models (Eqn 4) for a variety of measurements of thermal history ($T_{hist}$). $T_{hist}$ represented the ambient temperature at the time of measurement ($T_{amb}$), running averages of temperature ranging from 1 to 24 h ($T_{running1} - T_{running24}$), the

 

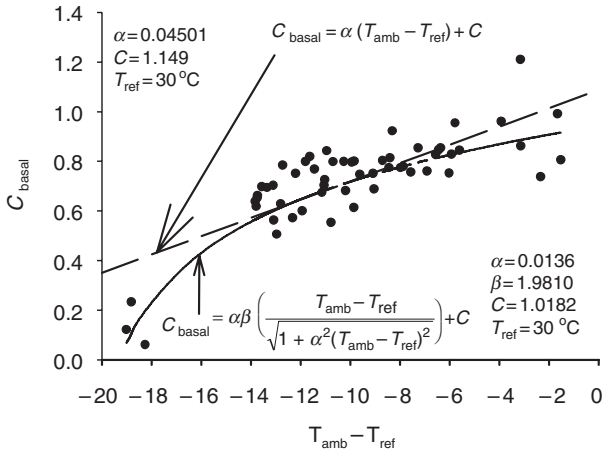


**Figure 1.** Fit of $C_{basal}$ correction algorithms to $C_{basal}$ factors calculated from MBO emission data collected in 2000. $C_{basal}$ correction factors (closed circles) were calculated by normalizing the MBO basal emission measured from four *Pinus ponderosa* saplings in 2000 to a value of 1 at 30 °C. $C_{basal}$ values are plotted against the departure of ambient temperature from a reference temperature ($T_{ref}$ = 30 °C). The broken line is a least squares linear regression fit to the $C_{basal}$ data ($C_{basal} = \alpha x + C$, where $x = T_{amb} - T_{ref}$). The solid line is a least squares regression for the non-linear model described in Eqn 5.

maximum temperature of the previous day ($T_{max-1}$), the minimum temperature of the previous night ($T_{min-1}$), the maximum temperature of two days prior ($T_{max-2}$), or the minimum temperature of two nights prior ($T_{min-2}$). Although linear models provided a good fit to most of the data (Fig. 1) they tended to overestimate emissions at low temperatures. In an attempt to take this observation into account we fit a non-linear model (Eqn 5) to the $C_{basal}$ data as shown in Fig. 1.

$$C_{basal} = \alpha\beta\left(\frac{T_{amb} - T_{ref}}{\sqrt{1 + \alpha^2 (T_{amb} - T_{ref})^2}}\right) + C \quad (5)$$

Two component models ($T_{hist1}$,$T_{hist2}$) incorporated measurements of temperature history on two time scales, or included both maximum and minimum temperature, and followed the form of Eqn 6, where $\alpha$, $\beta$ and $C$ are constants, $T_{hist1}$ is a short-term temperature component, $T_{hist2}$ is a long-term temperature component and $T_{ref}$ is a fixed reference temperature set at 30 °C. The short-term components $T_{hist1}$ comprised the ambient temperature at the time of measurement ($T_{amb}$) or the maximum temperature of the previous day ($T_{max-1}$). The long-term temperature components $T_{hist2}$ comprised averages of daily maximum temperature for the previous 2, 7 or 14 d ($T_{max2}$, $T_{max7}$, $T_{max14}$), or the minimum temperature of the previous 24 h ($T_{min}$).

$$C_{basal} = \alpha\left(\frac{T_{hist1}}{T_{ref}}\right) + \beta\left(\frac{T_{hist2}}{T_{ref}}\right) + C \quad (6)$$

## Model parameterization

The models describing the basal emission rate correction factor $C_{basal}$ were parameterized using MBO flux data and needle temperatures collected on four *P. ponderosa* saplings in the summer of 2000. Measurements were made between 10 June 2000 and 22 October 2000 with a 15 d sequence of daily measurements made between 4 July 2000 and 18 July 2000. All measurements on a tree were made on the same branch, and during the 15 d sequence of daily measurements the same set of needles was sampled to minimize the potentially confounding influence of branch and needle level variability in basal emission rate.

The MBO basal emission rate data obtained from the four trees in 2000 were first normalized to a value of $C_{basal} = 1$ when thermal history was equal to the standard temperature history reference temperature ($T_{ref}$ = 30 °C). This was done by fitting regression models (single-component and two-component) to the MBO basal emission data separately for each tree, and using the resulting equations to calculate the expected basal emission rate ($E_{standard30}$) at a temperature history of 30 °C. Dividing each measured MBO basal emission rate ($E_{basal}$) by this $E_{standard30}$ (where $T_{hist}$, $T_{his1}$ and $T_{hist2}$ = 30 °C) converts $E_{basal}$ to $C_{basal}$ (see Eqn 3). These $C_{basal}$ estimates for each tree were then pooled and used to fit the single-component (Eqns 4 & 5) and two-component (Eqn 6) $C_{basal}$ prediction equations.

## Model evaluation

We assessed the performance of the modified ISO G93 algorithm (Eqn 2) and the $C_{basal}$ correction algorithms (Eqns 4–6) by comparing measured MBO fluxes and the predicted MBO fluxes for two sets of data collected in 1998 and described in detail in Gray *et al.* (2003). The first set of data (seasonal) comprises MBO emission measurements made on age 0, age 1 and age 2 needles of a population of eight *P. ponderosa* saplings over the course of the growing season between 23 June and 14 October 1998. The second set of data (daily) comprises MBO emission measurements made on 1-year-old needles from a single tree between 23 June and 14 October 1998, and includes a 14 d sequence of daily measurements made between 28 July and 9 August 1998. The ratio of predicted : measured flux was calculated for each $C_{basal}$ model according to Eqn 7. Air temperatures were obtained from a nearby eddy flux/meteorology tower described in Lamanna & Goldstein (1999) and Goldstein *et al.* (2000).

$$\text{Departure} = \left(\frac{\text{Predicted MBO flux}}{\text{Measured MBO flux}}\right) \quad (7)$$

To obtain model output (predicted $E_{amb}$) we first calculated the $C_{basal}$ corresponding to each measured MBO flux using Eqns 4–6. Rearranging Eqn 3 we then divide each measured $E_{basal}$ by the corresponding $C_{basal}$ to obtain an estimate of $E_{standard30}$ for that measurement. Averaging these estimates of $E_{standard30}$ controls for errors in measurement of

$E_{basal}$, and the resulting average $E_{standard30}$ (Eqn 8) provides the $E_{standard30}$ input for Eqn 2. Using Eqn 2 to apply $C_L$, $C_T$ and $C_{basal}$ correction factors associated with each measured MBO emission rate results in a predicted MBO emission rate ($E_{amb}$). By combining Eqn 2 and Eqn 8 one obtains a general model (Eqn 9) for predicting MBO emission under ambient conditions ($E_{amb}$) from knowledge about $E_{basal}$, the thermal history associated with those $E_{basal}$ measurements, and the thermal history associated with the $E_{amb}$ one wants to predict. In Eqn 9, $E_{amb(y)}$ is the MBO emission rate under ambient conditions at time y, $C_{L(y)}$ and $C_{T(y)}$ are terms correcting for the instantaneous light and temperature response of MBO emission at time y, $C_{basal(y)}$ is the basal emission correction factor calculated to correct for thermal history at time 'y', $E_{basal(x)}$ and $C_{basal(x)}$ are the measured basal emission rate and basal emission rate correction factors obtained from samples taken at time 'x'.

$$E_{standard30} = \frac{1}{j}\sum_{1}^{j}\frac{E_{basal(x)}}{C_{basal(x)}} \quad (8)$$

$$E_{ambient(y)} = \frac{1}{j}\sum_{1}^{j}\frac{E_{basal(x)}}{C_{basal(x)}} C_{L(y)}C_{T(y)}C_{basal(y)} \quad (9)$$

## RESULTS

### Effect of thermal history on MBO basal emission

Examining the pattern of seasonal changes in MBO basal emission rate in both the 1998 and 2000 data sets clearly shows that MBO basal emission rates are not constant. Rather, MBO basal emission rates were low at the beginning of the season, increased to a peak in mid-season and subsequently declined towards the end of the growing season (Fig. 2) following a pattern of changes in MBO emission rates that closely paralleled the trajectory of seasonal changes in ambient temperature (Fig. 2). This pattern was most noticeable in the 1998 data set (Fig. 2a) but more difficult to recognize in the 2000 data set owing to the highly unstable weather following Day 240 in 2000. Examining the relationship between ambient temperature and basal MBO emission rate in the 2000 data set shows that basal MBO emission rates are linearly related with ambient temperature over most of their range (Fig. 1). However, at low temperatures there is a notable departure from linearity in which measured MBO basal emission rates are lower than expected.

### Daily performance: single-component models

Single-component models predicting MBO emission rates were based on thermal history measured at a single time scale ranging from hours to days. Regression parameters for single component models are shown in Table 1. Applying $C_{basal}$ models using the ambient air temperature at the time of each emission measurement ($T_{amb}$) or using thermal averaging windows of 1–24 h preceding each emission measurement ($T_{running1–24}$), resulted in patterns of predicted emission rates that were similar to the observed emission

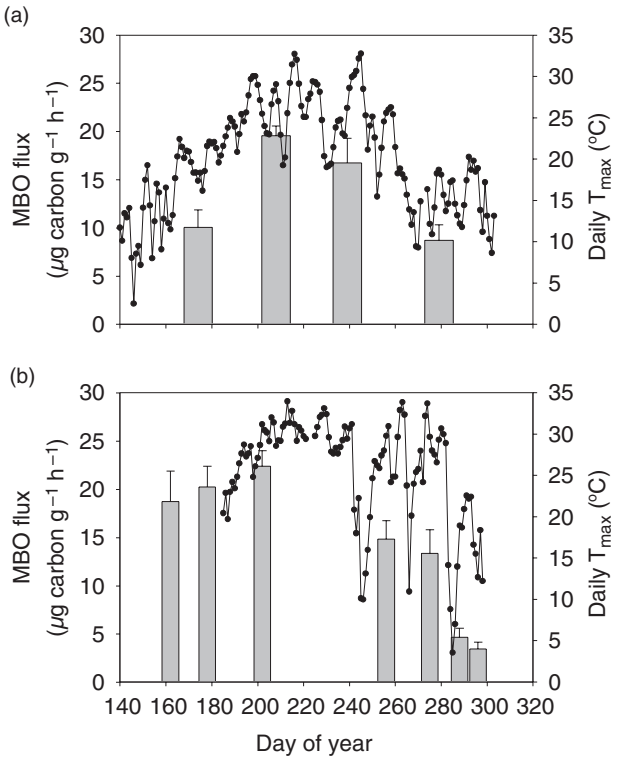


**Figure 2.** Seasonal patterns of daily maximum ambient temperature ($T_{max}$) and methylbutenol (MBO) basal emission rate in 1998 (a) and 2000 (b). In 1998 (a), MBO emission rates represent averages of 16 measurements taken on 1-year-old needles from eight *Pinus ponderosa* saplings. In 2000 (b), MBO basal emission rates are averages of 12 measurements of 1-year-old needles taken from four *P. ponderosa* saplings. Daily $T_{max}$ was obtained from an on-site meteorological tower in 1998 and from portable data loggers equipped with thermocouples located near the sampled trees in 2000. In 2000, two measurements of MBO basal emission rate took place prior to the onset of temperature data collection. Data were collected at standard measurement conditions of 1500 $\mu$mol photons $m^{-2}s^{-1}$ photosynthetic photon flux density (PPFD) and 30 °C needle temperature. Error bars represent ± 1 SE.

rates; however, these predicted emission rates were offset by up to 24 h, relative to the observed leaf-level emission levels (Fig. 3a). Among these models, the $T_{amb}$ model showed the greatest departure from observed emission rates exhibiting an amplitude of predicted emission rates that exceeded that observed in the data (Fig. 3a). Increasing the thermal averaging window from 1 to 24 h progressively improved the amplitude of the predicted emissions, although the 24 h shift in predicted emission rates remained (Fig. 3a). Similar results were obtained by applying the single component non-linear ($T_{ambnonlin}$) $C_{basal}$ model (Fig. 3b). Under the non-linear model predicted emission rates were shifted by up to 24 h; and although the amplitude of MBO emission rates predicted using the $T_{ambnonlin}$ model fit the observed data better than the linear $T_{amb}$ model, the more complicated non-linear model did not appear to provide better predictions than a 24 h running average of ambient temperature (Fig. 3a & b).

 

**Table 1.** Regression parameters for single-component models predicting the basal emission rate correction factor $C_{basal}$ from various measures of temperature history

| Thermal history parameter | Slope | Intercept | Correlation coefficient |
|---|---|---|---|
| $T_{amb}$ | 0.04501 | 1.149 | 0.752 |
| $T_{running1}$ | 0.04522 | 1.136 | 0.778 |
| $T_{running2}$ | 0.04116 | 1.089 | 0.761 |
| $T_{running3}$ | 0.03170 | 1.020 | 0.669 |
| $T_{running4}$ | 0.02572 | 0.973 | 0.596 |
| $T_{running5}$ | 0.02406 | 0.965 | 0.600 |
| $T_{running6}$ | 0.02292 | 0.957 | 0.605 |
| $T_{running7}$ | 0.02395 | 0.959 | 0.675 |
| $T_{running8}$ | 0.02288 | 0.966 | 0.643 |
| $T_{running12}$ | 0.02310 | 0.872 | 0.730 |
| $T_{running18}$ | 0.03430 | 1.079 | 0.837 |
| $T_{running24}$ | 0.02848 | 1.024 | 0.692 |
| $T_{max-1}$ | 0.04602 | 1.027 | 0.869 |
| $T_{max-2}$ | 0.03716 | 1.044 | 0.800 |
| $T_{min-1}$ | 0.03556 | 1.179 | 0.822 |
| $T_{min-2}$ | 0.03391 | 1.180 | 0.796 |

Notes: Parameters were related through the linear model $C_{basal} = \alpha(T_{hist} - T_{ref}) + C$ where $C_{basal}$ = the basal emission rate correction factor, $T_{hist}$ = the measure of thermal history, $T_{ref}$ = a reference temperature set to 30 °C, $\alpha$ = slope and $C$ = intercept. $T_{amb}$ = ambient temperature measured at the time of emission measurement, $T_{running1-24}$ = running averages of temperature measured over 1–24 h, $T_{max-1}$ and $T_{min-1}$ are the maximum and minimum temperature of the previous day, respectively, and $T_{max-2}$ and $T_{min-2}$ are the maximum and minimum temperatures of two days prior, respectively.

Single-component models incorporating lag effects for temperature (e.g. minimum or maximum temperature of previous days) predicted changes in MBO emission rates poorly, exhibiting both large amplitudes and temporal offsets. $C_{basal}$ models parameterized for either the minimum or the maximum temperature of the previous 24 h ($T_{min}$ or $T_{max-1}$) resulted in predicted MBO emission rates that were offset by 1–2 d (Fig. 3b), while models parameterized for either the minimum or maximum temperature of two days prior to the emission measurement resulted in a pattern of predicted emissions that was offset by 2–3 d (data not shown). When adjusted for these temporal offsets, the amplitude of predicted emission rates still exceeded that of the observed emission rates for all minimum or maximum temperature models (Fig. 3b), and was no better than the models based on running averages of temperature (Fig. 3a).

## Daily performance: two-component models

Two-component models predicting MBO emission rates were based either on measurements of thermal history at two timescales (hourly and daily) or were based on measurements of both the ambient temperature at the time of emission measurement and the lowest temperature of the previous 24 h. Regression parameters for two-component models are shown in Table 2. Adding a longer-term measurement of temperature history (daily/weekly average maximum temperature) to the single-component models previously examined improved the amplitude of predicted MBO emissions over the predictions of the parent single-component model. However, most models retained the single-component parent model's temporal shift of predicted MBO emission rates (Fig. 3c).

The sole exception was the $T_{amb}$ model which, upon inclusion of the temperature averages over multiple days in

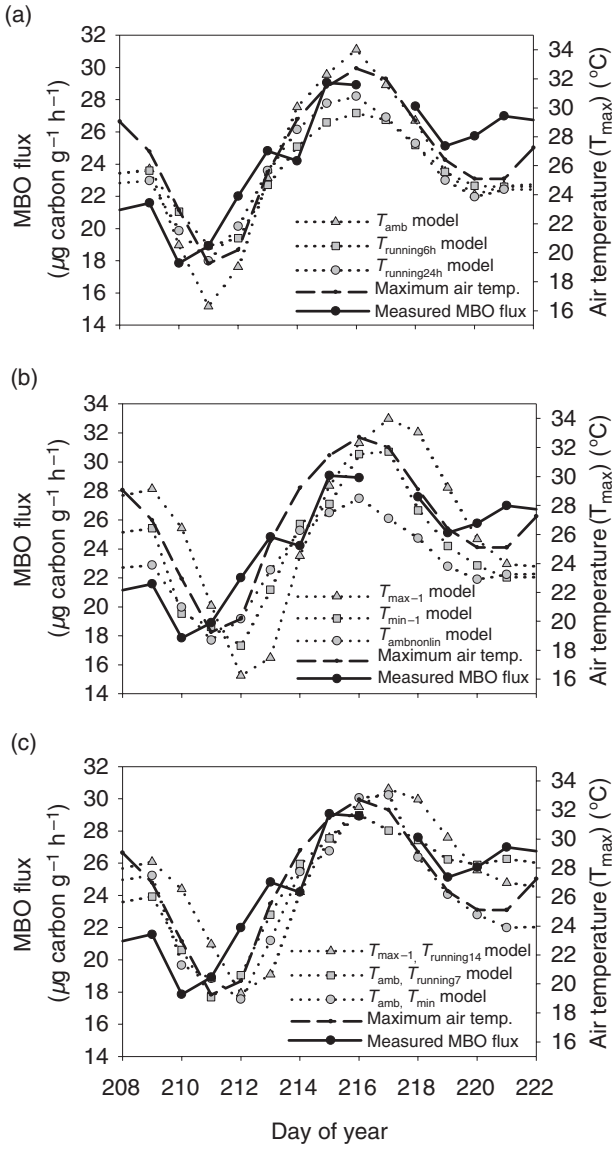


**Figure 3.** Comparison of selected single-component models (a & b) and two-component models (c) used to predict basal methylbutenol (MBO) emission rates. Fine-scale changes in MBO basal emission rate for a single tree shown over a 14 d period between 28 July and 9 August 1998. No emission measurements were made on day of year 217. Daily maximum temperature is plotted as a dashed line. Measured MBO basal emission rates are shown in closed circles and a solid line. Modelled MBO basal emission rates are shown in grey symbols and dotted lines. Basal MBO emission rates were collected at standard measurement conditions of 1500 $\mu$mol photons $m^{-2}s^{-1}$ photosynthetic photon flux density (PPFD) and 30 °C needle temperature.

**Table 2.** Regression parameters for two-component models predicting the basal emission rate correction factor $C_{basal}$ from various measures of temperature history

| Thermal history parameter | | | | | |
|---|---|---|---|---|---|
| $T_{hist1}$ | $T_{hist2}$ | $\alpha$ | $\beta$ | $C$ | Correlation coefficient |
| $T_{max-1}$ | $T_{max2}$ | 0.030 | 1.371 | –0.401 | 0.978 |
| | $T_{max7}$ | 1.568 | –0.135 | –0.430 | 0.986 |
| | $T_{max14}$ | 0.922 | 0.668 | –0.589 | 0.983 |
| | $T_{min-1}$ | 0.911 | 0.284 | –0.215 | 0.972 |
| $T_{amb}$ | $T_{max2}$ | 0.497 | 0.960 | –0.428 | 0.876 |
| | $T_{max7}$ | 0.822 | 0.805 | –0.601 | 0.980 |
| | $T_{max14}$ | 0.709 | 0.963 | –0.672 | 0.988 |
| | $T_{min-1}$ | –0.010 | 0.950 | 0.133 | 0.979 |

Notes: Parameters were related through the model $C_{basal} = \alpha(T_{hist1}/T_{ref}) + \beta(T_{hist2}/T_{ref}) + C$ where $C_{basal}$ = the basal emission rate correction factor, $T_{hist1}$ = the short-term measure of thermal history, $T_{hist2}$ = the longer-term measure of thermal history. $T_{amb}$ = ambient temperature measured at the time of emission measurement, $T_{max-1}$ is the maximum of the previous day, $T_{max2}$ is the average maximum temperature of the previous 2 d, $T_{max7}$ is the average maximum temperature of the previous 7 d, $T_{max14}$ is the average maximum temperature of the previous 14 d, $T_{min-1}$ is the minimum temperature of the previous 24 h, $T_{ref}$ is a reference temperature set to 30 °C.

addition to the hourly measurement of thermal history, exhibited nearly a perfect match between the periodicity of predicted and observed MBO emission rates (Fig. 3c). The match between the amplitude of these predictions and the observed emission rates improved with the length of averaging interval such that the $T_{amb}$,$T_{max7}$ and $T_{amb}$,$T_{max14}$ models exhibited nearly a perfect match between both the period and amplitude of predicted and observed MBO emission rates (Fig. 3c), rendering these the best two models examined. In contrast, the amplitude of emissions predicted by the $T_{amb}$,$T_{max2}$ model exceeded those of the parent single-component $T_{amb}$ model (data not shown).

MBO emission rates predicted under the two-component $T_{amb}$,$T_{min}$ model closely followed the amplitude of observed MBO emission rates; however, predicted emissions were offset from the observed data by 2 d (Fig. 3c).

## Seasonal performance of emission prediction algorithms

Figure 4 illustrates the performance, measured as the ratio of modelled MBO emission rates to measured MBO emission rates, of selected models applied to the 1998 population level data set. Failing to correct for changes in basal emission rate (Eqn 1) resulted in dramatic overestimates of MBO emission in both early and late season (36% and 74%), and smaller underestimates of MBO emission during mid-season (–9.6% and –16.8%). Adding a $C_{basal}$ term to the MBO emission prediction algorithm (Eqn 2) improved model predictions for all $C_{basal}$ thermal history correction algorithms examined. Regression parameters for these models are shown in Tables 1 and 2.

Among the single component models, those parameterized for $T_{amb}$ and $T_{running1–24}$ offered improved fit to the observed emission rates, but still underestimated emission rates during mid-season while overestimating emission rates during both early and late season. These overestimates increased as the length of the averaging window increased from 1 to 24 h (Fig. 4a). Similar results were obtained for the non-linear model (Fig. 4b), which also

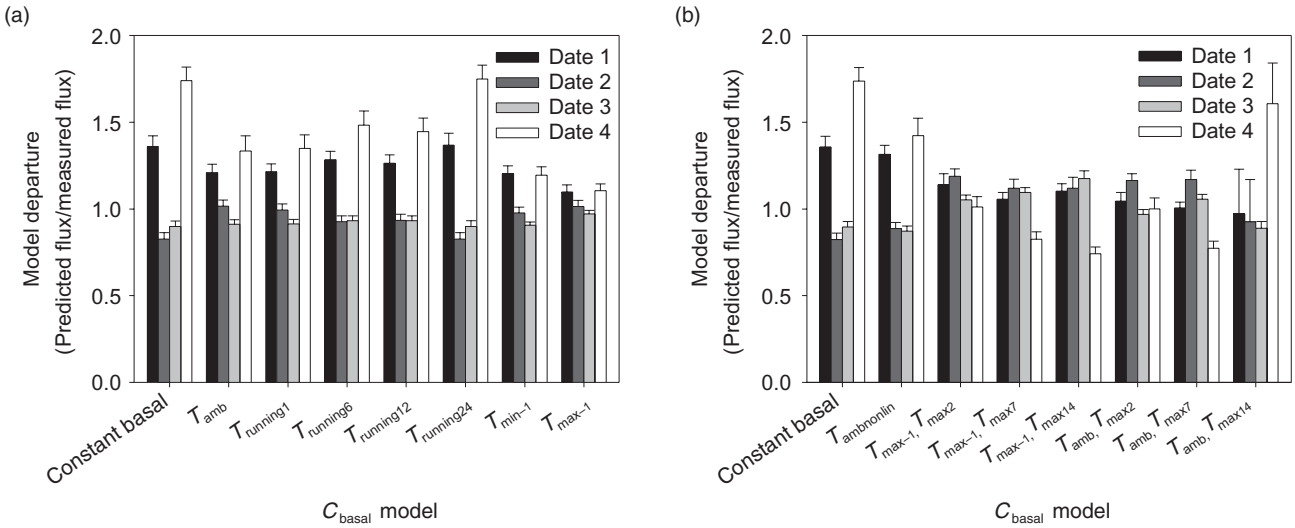


**Figure 4.** Departure of methylbutenol (MBO) basal emission rates predicted using various $C_{basal}$ emission rate correction factor algorithms from MBO basal emission rates measured throughout the season in 1998. Date 1 = days 174–183, date 2 = days 208–221, date 3 = days 239–253 and Date 4 = days 279–287. The constant basal model held MBO basal emission rate constant, while all other models allowed MBO basal emission rate to change through the application of a $C_{basal}$ term in Eqn 2. (a) shows the performance of selected single component models. (b) shows the performance of two-component models and the non-linear model for ambient temperature. Basal MBO emission rates were collected at standard measurement conditions of 1500 $\mu$mol photons $m^{-2}s^{-1}$ photosynthetic photon flux density (PPFD) and 30 °C needle temperature. Error bars represent ± 1 SE. $n = 8$ *Pinus ponderosa* individuals.

 

underestimated mid-season emission rates by (11–12%) and overestimated early and late season emission rates by (32% and 43%). Despite their poor performance in predicting day-to-day changes in emission rates (Fig. 3b), the $C_{basal}$ models parameterized for daily maximum or minimum temperature provided a close fit to the observed seasonal emission rates (Fig. 4a).

$C_{basal}$ models correcting for thermal history at two timescales (two-component models, Eqn 6) all performed better than assuming a constant basal emission rate using Eqn 1 (Fig. 4b). These models generally provided good predictions of the observed emission rates with slight overestimates in early and mid season, and marginally larger underestimates during late season. The $T_{amb}$,$T_{max14}$ model was an exception to this pattern and overestimated late season emissions by 61%. Among the two-component models the best seasonal performance was provided by the $T_{amb}$,$T_{max2}$ model; however, this model was only slightly better than the other two-component models (Fig. 4b).

## DISCUSSION

### Implications for modelling MBO emission

Of the single-component $C_{basal}$ correction algorithms examined in this study, models parameterized for $T_{min}$ or $T_{max}$ of the previous 1 or 2 d provided the greatest improvement in MBO prediction in the population data set. This result corresponds well with those of Sharkey *et al*. (1999), which showed that the temperature of the previous 1–2 d gave good predictions of observed isoprene emission rates. However, examining the performance of the single-component MBO emission rate prediction models in a more detailed fashion using the single-tree data set shows that the $T_{min}$ and $T_{max}$ models performed poorly at predicting MBO emission rates in early and late season, and that a model based on very recent measurements of thermal history ($T_{amb}$) provided a better fit to the day-to-day changes in MBO basal emission rate than did models based on either $T_{max}$ or $T_{min}$.

Adding a second temperature history component (average daily maximum temperature of the previous 2–14 d, or the minimum temperature of the previous 24 h) to form a two-component model improved early season performance of both $T_{amb}$ and $T_{max}$ containing models, and is consistent with the improved predictions Fuentes & Wang (1999) obtained with a model using cumulative degree days. However, despite the good seasonal performance of the two-component models containing $T_{max–1}$ as the short-term history component, these models failed to match observed day-to-day changes in MBO basal emission (Fig. 3c) and exhibited temporal offsets of 1–3 d. In contrast, the two-component models containing $T_{amb}$ as the short-term temperature history component matched observed day-to-day changes in MBO basal emission very closely and offered improvement over the single-component $T_{amb}$ model in seasonal (especially early season) predictions (Fig. 4b). Thus, we recommend that future attempts to predict MBO emissions should use one of the two-component models incorporating $T_{amb}$ as the short-term temperature history component. This set of models is remarkably similar to the model developed for isoprene by Guenther, Baugh & Brasseur (1999), which showed that basal isoprene emission rates were best predicted by a two-component model using the temperature of the previous 1 h and 15 d as inputs.

However, deciding among $T_{max2}$, $T_{max7}$, or $T_{max14}$ as the longer-term temperature history component ($T_{hist2}$) is difficult because different models perform best at different timescales. Although the $T_{amb}$,$T_{max2}$ model provides the best prediction for seasonal changes, the $T_{amb}$,$T_{max2}$ model was clearly outperformed by the $T_{amb}$,$T_{max7}$ and $T_{amb}$,$T_{max14}$ models for predicting day-to-day changes in basal MBO emission. Because the $T_{amb}$,$T_{max2}$ model exhibited both a 24 h offset in emission predictions as well as a larger than observed amplitude of emission rate change, it seems that this model has failed to capture some aspect of the response to thermal history (possibly too short a temperature averaging time) and that the $T_{amb}$,$T_{max7}$ and $T_{amb}$,$T_{max14}$ models may be expected to better represent the underlying biology of changes in MBO basal emission rates. In deciding between the $T_{amb}$,$T_{max7}$ and $T_{amb}$,$T_{max14}$ MBO basal emission correction models, the very large departure of predicted late season emission from observed emission rates under the $T_{amb}$,$T_{max14}$ model (Fig. 4b) suggests that the best $C_{basal}$ algorithm is the $T_{amb,}$ $T_{max7}$ model.

The models examined in this study were limited to investigating the role of temperature on MBO basal emission rates. However, Sharkey *et al*. (1999) showed that for predicting isoprene basal emission rates a model incorporating averages of both temperature and incident PAR gave better predictions than temperature alone. Although influences of photosynthetically active radiation (PAR) were not examined in this study, it is unlikely that PAR plays an important role in regulating basal MBO emission rates. Gray, Goldstein & Lerdau (2005) demonstrated through experimental shading that light environment had no detectable influence on basal MBO emission rates. This difference between isoprene and MBO may stem from the influence light has upon leaf temperature in broadleaf plants versus conifer needles. When illuminated, the foliage of broadleaf plants can rapidly increase to as much as 6–7 °C greater than the surrounding air temperature (Singsaas & Sharkey 1998). In contrast, in conifers needle temperatures are strongly coupled to air temperature and show negligible differences even under direct sunlight (Gray *et al*. 2005). Because most isoprene-emitting species possess broadleaf foliage, the model improvement Sharkey *et al*. (1999) obtained by adding a PAR term to the temperature model may be a result of the PAR term capturing the effect of indirect leaf heating rather that a direct effect of light.

Although parameterized for MBO-emitting pines, the basal emission correction algorithm described in this study may also be applicable for isoprene-emitting species, subject to the limitation that this model does not predict the absence of isoprene emission from young foliage. Unlike isoprene-emitting broadleaf plants, the foliage of MBO-

emitting pines exhibits no developmental delay in MBO emission (Lerdau & Gray 2003). Applying this model to predict isoprene fluxes following the onset of isoprene emission would serve as a robust test of the generality of the ambient temperature correction algorithm and provide support for the existence of a common underlying mechanistic basis for the temperature response.

### Regulation of MBO basal emission

The present study illustrates three important points about MBO basal emission. Firstly, that MBO emission rates change through the season, secondly, that these changes can be modelled as a function of temperature history, and thirdly, that MBO basal emission rates appear to be regulated at two timescales (hourly and daily). However, the mechanism underlying these seasonal changes remains uncertain. Elucidating the mechanism responsible for the observed changes in MBO emission rates is complicated by the fact that two potential controls over MBO emission (temperature and photosynthetic rates) were changing concurrently during both field studies examined in this study.

Work by Zimmer *et al*. (2000) has shown that modelling the supply of carbon substrates derived from photosynthesis can lead to accurate predictions of diurnal isoprene emission patterns. By extrapolation, one might predict that as drought reduces photosynthetic capacity in MBO-emitting foliage, MBO emission rates should also decline, because MBO biosynthesis takes place in the chloroplast and is linked to the Calvin cycle through the DOXP/MEP pathway (Rohmer *et al*. 1993; Lichtenthaler 1999). However, while substrate limitation is consistent with the observed late-season decline in MBO emission, it does not explain the low emission rates observed early in the season when photosynthetic rates (and presumably carbon availability) are at their seasonal peak. A role of substrate limitation in explaining the seasonal pattern of basal MBO emission rates is further argued against by Gray *et al*. (2003), who found only a weak relationship between photosynthetic capacity and MBO basal emission rates, and Gray *et al*. (2005), who found that shading had no effect on MBO basal emission rates. Together, these results suggest that changes in substrate availability do not control seasonal changes in MBO emission rates.

Instead it seems likely that these changes in basal emission rates are a result of the changes in the amount of the enzyme (MBO synthase) responsible for producing MBO (Fisher *et al*. 2000) present in MBO-emitting foliage. This hypothesis is consistent with the observation that isoprene synthase activity changes in tandem with basal isoprene emission rate in *Quercus robur* (Schnitzler *et al*. 1997). The induction of heat shock protein biosynthesis in plants exposed to high temperatures demonstrates that plants possess the capacity to sense their thermal environment and to change their biochemical composition in response (Vierling 1991; Heckathorn *et al*. 1998); thus it is possible that MBO synthase content may be regulated by temperature in a similar fashion. Such a possibility is intriguing given the similar biosynthetic origin and ecophysiological regulation of MBO and isoprene, and the hypothesized function of isoprene in protecting plants from damage at high temperatures (Sharkey & Singsaas 1995; Singsaas *et al*. 1997; Sharkey, Chen & Yeh 2001). For plants to up-regulate their capacity to biosynthesize a costly thermal protectant during warm weather and then to down-regulate this capacity during cooler weather, as observed in this study, is entirely consistent with a hypothesis of MBO possessing a role in high temperature thermal protection, although it does not inform about the physiological mechanism that might account for such protection.

## CONCLUSIONS

At present the proposed model for predicting changes in basal MBO emission rates is surely a crude representation of the biology underlying these changes; and many important questions remain unanswered. Notably, a better understanding of how basal emission rate responds to temperature extremes (both high and low) is needed, as is an examination of the relative rates of up-regulation and down-regulation of basal MBO emission in response to the changes in ambient temperature. Much work awaits the development of the molecular tools that will allow one to directly address whether changes in MBO basal emission rates can be attributed to changes in the amounts of MBO biosynthetic enzymes. Until that time, greenhouse and growth chamber studies designed to address the dynamic response of MBO basal emission rates following temperature increases and decreases will surely add to our understanding of how MBO basal emission rates are regulated, and may help to clarify whether the control of MBO basal emission stems from changes in the rate at which MBO synthase is produced or in the rate at which it degrades.

## ACKNOWLEDGMENTS

This work was made possible by a NASA Earth System Science Fellowship to D.W. Gray. We thank the Blodgett Forest Research Station staff for their invaluable logistical support and Sierra Pacific Industries for allowing us to carry out research on their property. We especially thank Robert Heald for aid in selecting field sites, Russell Seufert for the use of the carpentry shop as summer research space for D.W. Gray, and Jeanne Panek and Gunnar Schade for many stimulating discussions. D.W. Gray also thanks the Forest Technicians for their innumerable contributions. Dianna Padilla provided useful comments on earlier versions of this manuscript. D.W. Gray would also like to acknowledge Sue Natali for housing D.W. Gray (thereby preventing homelessness) during manuscript preparation.

## REFERENCES

Andreae M.O. & Crutzen P.J. (1997) Atmospheric aerosols: biogeochemical sources and role in atmospheric chemistry. *Science* **276,** 1052–1058.

Brasseur G.P. & Chatfield R.B. (1991) The fate of biogenic trace gases in the atmosphere, In *Trace Gas Emissions by Plants* (eds T.D. Sharkey, E.A. Holland & H.A. Mooney), pp. 1–27. Academic Press, Inc., San Diego, CA, USA.

Chameides W.L., Fehsenfeld F., Rodgers M.O., *et al.* (1992) Ozone precursor relationships in the ambient atmosphere. *Journal of Geophysical Research* **97,** 6037–6055.

Ehhalt D.H., Dorn H.-P. & Poppe D. (1991) The chemistry of the hydroxyl radical in the troposphere. *Proceedings of the Royal Society of Edinburgh* **97B,** 17–34.

Fehsenfeld F., Calvert J., Fall R., *et al.* (1992) Emissions of volatile organic compounds from vegetation and the implications for atmospheric chemistry. *Global Biogeochemical Cycles* **6,** 389–430.

Fisher A.J., Baker B.M., Greenberg J.P. & Fall R. (2000) Enzymatic synthesis of methylbutenol from dimethylallyl diphosphate in needles of *Pinus sabiniana*. *Archives of Biochemistry and Biophysics* **383,** 128–134.

Fuentes J.D. & Wang D. (1999) On the seasonality of isoprene emissions from a mixed temperate forest. *Ecological Applications* **9,** 1118–1131.

Geron C., Guenther A., Sharkey T. & Arnts R.R. (2000) Temporal variability in basal isoprene emission factor. *Tree Physiology* **20,** 799–805.

Goldan P.D., Kuster W.C. & Fehsenfeld F.C. (1993) The observation of a $C_5$ alcohol emission in a North American pine forest. *Geophysical Research Letters* **20,** 1039–1042.

Goldstein A.H. & Schade G.W. (2000) Quantifying biogenic and anthropogenic contributions to acetone mixing ratios in a rural environment. *Atmospheric Environment* **34,** 4997–5006.

Goldstein A.H., Goulden M.L., Munger J.W., Wofsy S.C. & Geron C.D. (1998) Seasonal course of isoprene emissions from a midlatitude deciduous forest. *Journal of Geophysical Research* **103,** 31 045–31 056.

Goldstein A.H., Hultman N.E., Fracheboud J.M., Bauer M.R., Panek J.A., Xu M., Qi Y., Guenther A.B. & Baugh W. (2000) Effects of climate variability on the carbon dioxide, water, and sensible heat fluxes above a ponderosa pine plantation in the Sierra Nevada (CA). *Agricultural and Forest Meteorology* **101,** 113–129.

Gray D.W., Lerdau M.T. & Goldstein A.H. (2003) Influences of temperature history, water stress, and needle age on methylbutenol emissions. *Ecology* **84,** 765–776.

Gray D.W., Goldstein A.H. & Lerdau M.T. (2005) The influence of light environment on photosynthesis and basal methylbutenol emission rate from *Pinus ponderosa*. *Plant, Cell and Environment* **28,** 1463–1474.

Guenther A. (1997) Seasonal and spatial variations in natural volatile organic compound emissions. *Ecological Applications* **7,** 34–45.

Guenther A., Hewitt N.C., Erickson D., *et al.* (1995) A global model of natural volatile organic compound emissions. *Journal of Geophysical Research* **100,** 8873–8892.

Guenther A., Baugh B. & Brasseur G. (1999) Isoprene emission estimates and uncertainties for the Central African EXPRESSO study domain. *Journal of Geophysical Research – Atmospheres* **104,** 30 625–30 639.

Guenther A.B., Monson R.K. & Fall R. (1991) Isoprene and monoterpene emission rate variability: observations with *Eucalyptus* and emission rate algorithm development. *Journal of Geophysical Research* **96,** 10 799–10 808.

Guenther A.B., Zimmerman P.R. & Harley P.C. (1993) Isoprene and monoterpene emission rate variability: model evaluations and sensitivity analyses. *Journal of Geophysical Research* **98,** 12 609–12 617.

Harley P., Guenther A. & Zimmerman P. (1996) Effects of light, temperature, and canopy position on net photosynthesis and isoprene emission from sweetgum (*Liquidambar styraciflua*) leaves. *Tree Physiology* **16,** 25–32.

Harley P., Guenther A. & Zimmerman P. (1997) Environmental controls over isoprene emission in deciduous oak canopies. *Tree Physiology* **17,** 705–714.

Harley P., Fridd-Stroud V., Greenberg J., Guenther A. & Vasconcellos P. (1998) Emission of 2-methyl-3-buten-2-ol by pines: a potentially large natural source of reactive carbon to the atmosphere. *Journal of Geophysical Research* **103,** 25479–25486.

Harley P.C., Litvak M.E., Sharkey T.D. & Monson R.K. (1994) Isoprene emission from velvet bean leaves: interactions among nitrogen availability, growth photon flux density, and leaf development. *Plant Physiology* **105,** 279–285.

Heckathorn S.A., Downs C.A., Sharkey T.D. & Coleman J.S. (1998) The small, methionine-rich chloroplast heat-shock protein protects photosystem II electron transport during heat stress. *Plant Physiology* **116,** 439–444.

Jacob D.J. & Wofsy S.C. (1988) Photochemistry of biogenic emissions over the Amazon forest. *Journal of Geophysical Research* **93,** 1477–1486.

Kreuzweiser J., Schnitzler J.-P. & Steinbrecher R. (1999) Biosynthesis of organic compounds emitted by plants. *Plant Biology* **1,** 149–159.

Kuhn U., Rottenberger S., Biesenthal T., Wolf A., Schebeske G., Ciccioli P., Brancaleoni E., Frattoni M., Tavares T.M. & Kesselmeier J. (2004) Seasonal differences in isoprene and light-dependent monoterpene emission by Amazonian tree species. *Global Change Biology* **10,** 663–682.

Lamanna M.S. & Goldstein A.H. (1999) In situ measurements of $C_2$-$C_{10}$ volatile organic compounds above a Sierra Nevada ponderosa pine plantation. *Journal of Geophysical Research* **104,** 21247–21262.

Lehning A., Zimmer W., Zimmer I. & Schnitzler J.-P. (2001) Modeling of annual variations of oak (*Quercus robur* L.) isoprene synthase activity to predict isoprene emission rates. *Journal of Geophysical Research* **106,** 3157–3166.

Lerdau M. & Gray D. (2003) Ecology and evolution of light-dependent and light-independent phytogenic volatile organic carbon. *New Phytologist* **157,** 199–211.

Lichtenthaler H.K. (1999) The 1-deoxy-D-xylulose-5-phosphate pathway of isoprenoid biosynthesis in plants. *Annual Review of Plant Physiology and Plant Molecular Biology* **50,** 47–65.

Li-Cor (1995) *Technical Note 5: Energy Balance.* Li-Cor Inc., Lincoln, NB, USA.

Llusià J. & Peñuelas J. (2000) Seasonal patterns of terpene content and emission from seven Mediterranean woody species in field conditions. *American Journal of Botany* **87,** 133–140.

Loreto F. & Sharkey T.D. (1993) On the relationship between isoprene emission and photosynthetic metabolites under different environmental conditions. *Planta* **189,** 420–424.

MacDonald R.C. & Fall R. (1993a) Acetone emission from conifer buds. *Phytochemistry* **34,** 991–994.

MacDonald R.C. & Fall R. (1993b) Detection of substantial emissions of methanol from plants to the atmosphere. *Atmospheric Environment* **27A,** 1709–1713.

Monson R.K. & Fall R. (1989) Isoprene emission from aspen leaves: influence of environment and relation to photosynthesis and photorespiration. *Plant Physiology* **90,** 267–274.

Monson R.K., Hills A.J., Zimmerman P.R. & Fall R.R. (1991) Studies of the relationship between isoprene emission rate and $CO_2$ or photon-flux density using a real-time isoprene analyzer. *Plant, Cell and Environment* **14,** 517–523.

Monson R.K., Jaeger C.H., Adams W.W. III, Driggers E.M., Silver G.M. & Fall R. (1992) Relationships among isoprene emission

rate, photosynthesis, and isoprene synthase activity as influenced by temperature. *Plant Physiology* **98,** 1175–1180.

Monson R.K., Harley P.C., Litvak M.E., Wildermuth M., Guenther A.B., Zimmerman P.R. & Fall R. (1994) Environmental and developmental controls over the seasonal pattern of isoprene emission from Aspen leaves. *Oecologia* **99,** 260–270.

Nemecek-Marshall M., MacDonald R.C., Franzen J.J., Wojciechowski C.L. & Fall R. (1995) Methanol emission from leaves. *Plant Physiology* **108,** 1359–1368.

Novakov T. & Penner J.E. (1993) Large contribution of organic aerosols to cloud-condensation-nuclei concentrations. *Nature* **365,** 823–826.

Pétron G., Harley P., Greenberg J. & Guenther A. (2001) Seasonal temperature variations influence isoprene emission. *Geophysical Research Letters* **28,** 1707–1710.

Rohmer M., Knani M., Simonin P., Sutter B. & Sahm H. (1993) Isoprenoid biosynthesis in bacteria- A novel pathway for the early steps leading to isopentenyl diphosphate. *Biochemical Journal* **295,** 517–524.

Schade G.W., Goldstein A.H., Gray D.W. & Lerdau M.T. (2000) Canopy and leaf level 2-methyl-3-buten-2-ol fluxes from a ponderosa pine plantation. *Atmospheric Environment* **34,** 3535–3544.

Schnitzler J.P., Lehning A. & Steinbrecher R. (1997) Seasonal pattern of isoprene synthase activity in *Quercus robur* leaves and its significance for modeling isoprene emission rates. *Botanica Acta* **110,** 240–243.

Sharkey T.D. & Loreto F. (1993) Water stress, temperature, and light effects on the capacity for isoprene emission and photosynthesis of Kudzu leaves. *Oecologia* **95,** 328–333.

Sharkey T.D. & Singsaas E.L. (1995) Why plants emit isoprene. *Nature* **374,** 769.

Sharkey T.D., Singsaas E.L., Lerdau M.T. & Geron C.D. (1999) Weather effects on isoprene emission capacity and applications in emission algorithms. *Ecological Applications* **9,** 1132–1137.

Sharkey T.D., Chen X. & Yeh S. (2001) Isoprene increases thermotolerance of Fosmidomycin-fed leaves. *Plant Physiology* **125,** 2001–2006.

Singsaas E.L. & Sharkey T.D. (1998) The regulation of isoprene emission responses to rapid leaf temperature fluctuations. *Plant, Cell & Environment* **21,** 1181–1188.

Singsaas E.L., Lerdau M., Winter K. & Sharkey T.D. (1997) Isoprene increases thermotolerance of isoprene-emitting species. *Plant Physiology* **115,** 1413–1420.

Tingey D.T., Manning M., Grothaus L.C. & Burns W.F. (1979) The influence of light and temperature on isoprene emission rates from live oak. *Physiologia Plantarum* **47,** 112–118.

Tingey D.T., Evans R. & Gumpertz M. (1981) Effects of environmental conditions on isoprene emission from live oak. *Planta* **152,** 565–570.

Vierling E. (1991) The role of heat shock proteins in plants. *Annual Review of Plant Physiology & Plant Molecular Biology* **42,** 579–620.

Wuebbles D., Grant K., Connell P. & Penner J. (1989) The role of atmospheric chemistry in climate change. *Journal of the Air Pollution Contrological Association* **39,** 22–28.

Zimmer W., Bruggeman N., Emeis S., Giersch C., Lehning A., Steinbrecher R. & Schnitzler J.-P. (2000) Process-based modeling of isoprene emission by oak leaves. *Plant, Cell & Environment* **23,** 585–595.

Zimmerman P.R. (1979) Testing of hydrocarbon emissions from vegetation, leaf litter, and aquatic surfaces and development of a methodology for compiling biogenic emission inventories. Final Report in United States Environmental Protection Agency, Research Triangle Park.

*Received 3 May 2005; received in revised form 31 January 2006; accepted for publication 1 February 2006*

 